Magnesium Technology 2012
Edited by: Suveen N. Mathaudhu, Wim H. Sillekens, Neale R. Neelameggham, and Norbert Hort
TMS (The Minerals, Metals & Materials Society), 2012

Length Changes in Extruded Magnesium Alloy Bars Under Large Strain Free-End Torsion

H. Wang[1], P.D. Wu[1], K.W. Neale[2]
[1]Department of Mechanical Engineering, McMaster University
Hamilton, Ontario L8S 4L7, Canada
[2]Faculty of Engineering, University of Sherbrooke
Sherbrooke, Quebec J1K 2R1, Canada

Keywords: Crystal plasticity, Torsion, Texture, Magnesium Alloy

Abstract

We numerically study the large strain free-end torsion of extruded magnesium alloy bars based on the recently developed Elastic Visco-Plastic Self-Consistent (EVPSC) model, in which both slip and twinning contribute to plastic deformation. It is shown that the predicted second-order length change is very sensitive to the initial texture and texture evolution. Numerical results suggest that the free-end torsion test can provide an effective means for assessing the adequacy of polycrystal plasticity models for magnesium alloys.

Introduction

The torsion of circular bars in the region of large strain deformations is of considerable practical interest. In particular, a torsion test seems to be ideally suited for the experimental determination of material parameters in the range of large strains. The major advantage for this purpose over tensile tests is that deformations during torsion remain homogeneous in the axial direction until fracture, without showing strain localization in necks etc. A second, slightly more academic interest in large strain torsion relates to attempts to incorporate deformation-induced anisotropy into large strain plasticity models. It has been generally accepted that texture development, which is the prime source of anisotropy in metals, leads to axial strains in the case of specimens with free ends (see e.g. Swift [1]), or leads to axial stresses in specimens with axial constraints or fixed ends (see e.g. Montheillet et al. [2]). The prediction of these phenomena depends strongly on the constitutive model, in particular the description of anisotropic hardening (see e.g. Harren et al. [3], Neale et al. [4], Toth et al. [5], and Wu et al. [6]). Thus, the torsion test can provide an effective means for assessing the adequacy of constitutive models.

Extensive experimental and numerical research has been performed on large strain torsion for polycrystals with the Face Centered Cubic (FCC) and Body Centered Cubic (BCC) crystallographic structures. However, there are rare investigations on the torsion of polycrystalline materials with the Hexagonal Close Packed (HCP) crystallographic structure. Sanchez et al. [7] and Evans et al. [8] studied texture evolution during torsion by simulating simple shear. Barnett [9] experimentally studied the flow stress of AZ31 under torsion. Balasubramanian and Anand [10] numerically studied texture evolution and the mechanical response of titanium under fixed-end torsion of a circular tube by using the finite element method. Beausir et al. [11] experimentally and numerically studied the free-end torsion of AZ71 and pure magnesium. However, all these numerical studies on the large strain torsion of HCP polycrystals excluded twinning. Very recently, Wang et al. [12] studied the large strain fixed-end torsion of HCP polycrystalline solid bars based on the semi-analytical approach proposed by Neale and Shrivastava [13], and the visco-plastic self-consistent (VPSC) model developed by Molinari et al. [14] and Lebensohn and Tomé [15], in which both slip and twinning contribute to plastic deformation. It was shown that the predicted second-order axial force is very sensitive to the initial texture, texture evolution and the constitutive models employed.

In this paper, we numerically study the large strain free-end torsion of magnesium alloy AZ31 extruded bars by using a special purpose finite element designed by Wu and Van der Giessen [16]. All the simulations are based on the large strain elastic viscoplastic self-consistent (EVPSC) model for polycrystalline materials developed by Wang et al. [17], which includes both slip and twinning as plastic deformation mechanisms. Results are presented in terms of predicted torque responses and axial strains. The influences of initial texture and texture evolution on the axial strain are emphasized.

Constitutive Model

In this section, we briefly recapitulate the constitutive model we adopt throughout this paper, mainly for the purpose of definition and notation. For details we refer to Wang et al. [17].

The elastic constitutive equation for a crystal is:

$$\overset{\nabla}{\boldsymbol{\sigma}}^{*} = \boldsymbol{L} : \boldsymbol{d}^{e} - \sigma tr(\boldsymbol{d}^{e}) \tag{1}$$

where $\boldsymbol{L}$ is the fourth order elastic stiffness tensor, $\boldsymbol{d}^{e}$ is the elastic strain rate tensor and $\overset{\nabla}{\boldsymbol{\sigma}}^{*}$ is the Jaumann rate of the Cauchy stress $\boldsymbol{\sigma}$ based on the lattice spin tensor $\boldsymbol{w}^{e}$. The single crystal elastic anisotropy is included in $\boldsymbol{L}$ through the crystal elastic constants C_{ij}.

Plastic deformation of a crystal is assumed to be due to crystallographic slip and twinning on systems $(\boldsymbol{s}^{\alpha}, \boldsymbol{n}^{\alpha})$. Here, $\boldsymbol{s}^{\alpha}$ and $\boldsymbol{n}^{\alpha}$ are the slip/twinning direction and the direction normal to the slip/twinning plane for system α, respectively. In the present study we consider slip in the Basal <a> ($\{0001\}<11\bar{2}0>$), Prismatic <a> ($\{10\bar{1}0\}<11\bar{2}0>$) and Pyramidal <c+a> ($\{\bar{1}\,\bar{1}22\}<\bar{1}\,\bar{1}23>$) slip systems, and twinning in the $\{10\bar{1}2\}<\bar{1}011>$ tensile twin system (see Fig. 1).

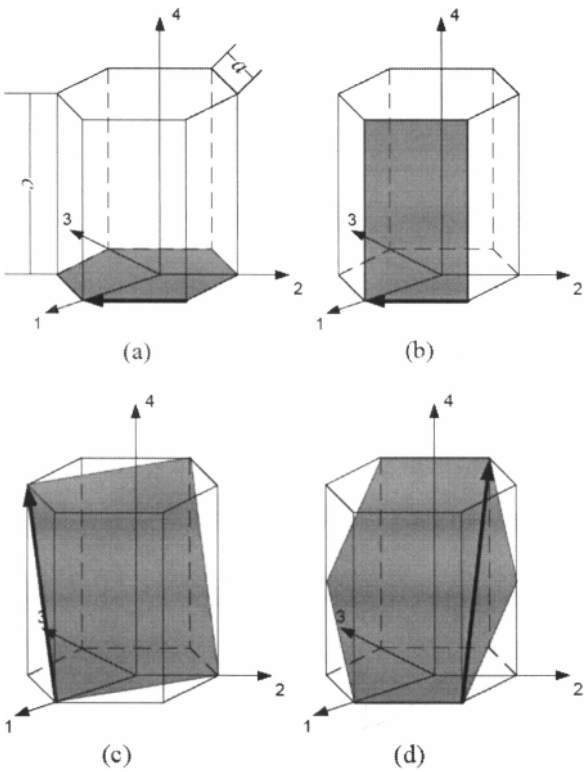

Figure 1. Plastic deformation modes for hexagonal structure: (a) basal <a> slip systems, (b) prismatic <a> slip systems, (c) pyramidal <c+a> slip systems, and (d) tensile twin.

The following equation gives the grain (crystal) level plastic strain rate:

$$\boldsymbol{d}^p = \dot{\gamma}_0 \sum_{\alpha} \boldsymbol{P}^{\alpha} \left| \frac{\tau^{\alpha}}{\tau^{\alpha}_{cr}} \right|^{\frac{1}{m}-1} \frac{\tau^{\alpha}}{\tau^{\alpha}_{cr}} \tag{2}$$

where $\dot{\gamma}_0$ is a reference value for the slip/twinning rate, m is the slip/twinning rate sensitivity, $\boldsymbol{P}^{\alpha} = (\boldsymbol{s}^{\alpha}\boldsymbol{n}^{\alpha} + \boldsymbol{n}^{\alpha}\boldsymbol{s}^{\alpha})/2$ is the Schmid tensor for system α, and $\tau^{\alpha} = \boldsymbol{\sigma} : \boldsymbol{P}^{\alpha}$ and τ^{α}_{cr} are the resolved shear stress and critical resolved shear stress (CRSS) for system α, respectively.

The self-consistent approach is applied to obtain the response of a polycrystal comprised of many grains. In a self-consistent approach each grain is treated as an ellipsoidal inclusion embedded in a Homogeneous Effective Medium (HEM), which is an aggregate of all the grains. Interactions between each grain and the HEM are described using the Eshelby inclusion formalism. During each deformation step, the single crystal constitutive rule (which describes the grain-level response) and the self-consistency criteria are solved simultaneously. This ensures that the grain-level stresses and strain rates are consistent with the boundary conditions imposed on the HEM. To date, various self-consistent schemes have been proposed. The EVPSC model for polycrystals recently developed by Wang et al. [17] is a completely general elastic-viscoplastic, fully anisotropic, self-consistent polycrystal model, applicable to large strains and to any crystal symmetry. Very recently, Wang et al. [12, 18-20] evaluated various linearization self-consistent schemes employed in self-consistent modeling by applying them to the large strain behavior of magnesium alloys under different deformation processes, including the fixed-end torsion of solid bars and forming limit diagrams. It was found that the Affine self-consistent scheme gave the best overall performance among the self-consistent approaches examined. Therefore, the EVPSC model with the Affine self-consistent scheme is applied in the present study. In addition, the Predominant Twin Reorientation (PTR) scheme proposed by Tomé et al. [21] is used to model the twinning activities.

Problem formulation and method of solution

We consider a solid circular bar with radius R_0 and length L_0 subjected to an angle of twist ψ due to an applied torque T. The lateral surface of the bar is stress free, and all properties are assumed to be axisymmetric and homogeneous along the axial direction. The end faces of the bar are constrained to the extent that they remain plane and perpendicular to the axial direction, so that we may assume that any cross-section of the bar remains planar. Although anisotropy will be induced during the deformation process, the behavior remains axisymmetric and the bar remains circular cylindrical with current radius R and current length L (Fig. 2). The bar is assumed to be in the free-end condition, thus allowing the possible development of a uniform axial displacement over the end face.

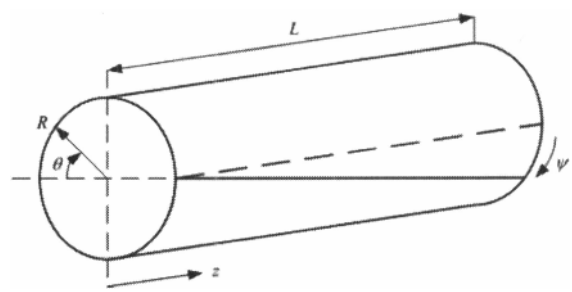

Figure 2. Schematic representation of a solid circular bar under torsion.

A numerical approach is adopted to solve the governing equations using a special purpose finite element developed by Wu and Van der Giessen [16, 22], and used by Van der Giessen et al. [23] and Wu et al. [6]. Each element effectively is a circular cylindrical tube, but computationally it is considered to be one-dimensional along the radial direction, with two nodes. The degrees of freedom of the entire finite element model of the bar consisting of n elements then comprise $n+1$ radial nodal displacements along with the axial displacement $U = L - L_0$ and the angle of twist ψ. Furthermore, each element has two material sampling points whose positions coincide with the Gaussian integration points. Each sampling point in the finite element formulation is modeled as a polycrystalline aggregate, and the EVPSC model with the Affine self-consistent scheme is applied locally at each sampling point. Finally, an equilibrium correction procedure is applied to prevent drifting of the solution from the true equilibrium path.

The results of large strain free-end torsion of a circular solid bar are efficiently presented in terms of the following quantities:

$$\Gamma = \frac{R_0}{L_0}\psi, \quad \bar{\tau} = \frac{3T}{2\pi R_0^3}, \quad \varepsilon = \ln\left(\frac{L}{L_0}\right) \qquad (3)$$

Here, Γ represents the shear strain at the outer surface of the bar, and $\bar{\tau}$ and ε are the normalized torque and axial strain, respectively.

Results and discussions

The material considered here is magnesium alloy AZ31 extruded bar, which has been experimentally studied by Agnew et al. [24]. The {0001} pole figure of the initial texture (Fig. 3) shows that the grains tend to have their basal planes oriented parallel (*c*-axis oriented perpendicular) to the extrusion direction (ED) of the bar. For a comparison, an initial random texture is also considered. The reference slip/twinning rate $\dot{\gamma}_0$ and the rate sensitivity m are prescribed to be the same for all slip/twinning systems: $\dot{\gamma}_0 = 0.001s^{-1}$ and $m = 0.05$, respectively. The room temperature elastic constants of magnesium single crystal are taken from Simmons and Wang [25] to be $C_{11} = 58.0$, $C_{12} = 25.0$, $C_{13} = 20.8$, $C_{33} = 61.2$ and $C_{44} = 16.6$ (units of GPa). Values of the hardening parameters for each mode are estimated by fitting numerical simulations of uniaxial tension and compression along the ED to the corresponding experimental flow curves.

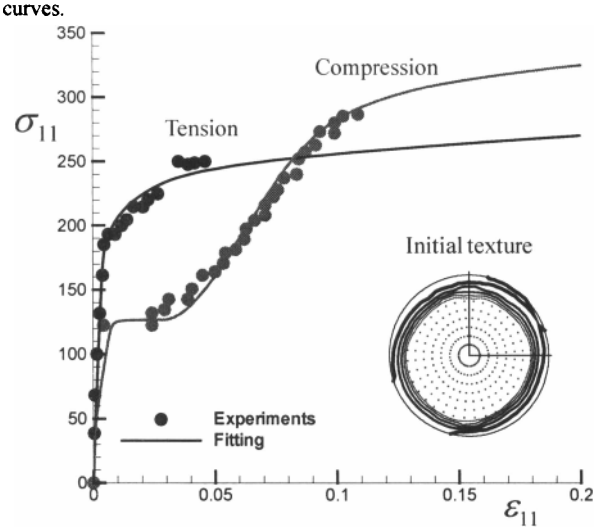

Figure 3. Stress and strain responses of AZ31 bar under uniaxial tension and compression along the ED. The insert is the initial texture represented in terms of the {0001} pole figure. The reflecting surface is normal to the ED.

The uniaxial tension and compression true stress - true strain curves along the ED are presented in Fig. 3. The characteristic S-shape of the compressive flow curve clearly reveals the importance of twinning in compression. The macroscopic yield stresses for uniaxial compression and tension are about 120 MPa and 190 MPa, respectively, showing the strong tension/compression asymmetry associated with twinning. The EVPSC model with the Affine self-consistent scheme fits the experimental curves quite well. The values of these parameters will be used in subsequent simulations.

We proceed by simulating large strain free-end torsion of solid bars with the initial extrusion texture and random texture. Calculations are carried out for solid bars with $R_0 = 1\,\text{mm}$ and $L_0 = 1\,\text{mm}$. For the fixed-end torsion of solid bars, Van der Giessen et al. [23] found, by comparison with the semi-analytical method (Neale and Shrivastava [13]), that sufficiently accurate results were obtained by using only $n = 5$ elements. Figure 4 shows stress distributions inside the solid bar with the initial random texture under free-end torsion at $\Gamma = 1.5$. These results are based on two meshes with 5 and 15 elements, respectively. It is found that the two meshes give very similar stress distributions. Although not shown here, the differences in the predicted $\bar{\tau}$ and ε between 5 and 15 elements are found to be very small. These observations suggest that using a mesh with 5 elements is also sufficient to accurately simulate the free-end torsion of solid bars. However, all the numerical results reported in the present study are based on a mesh with $n = 10$ elements.

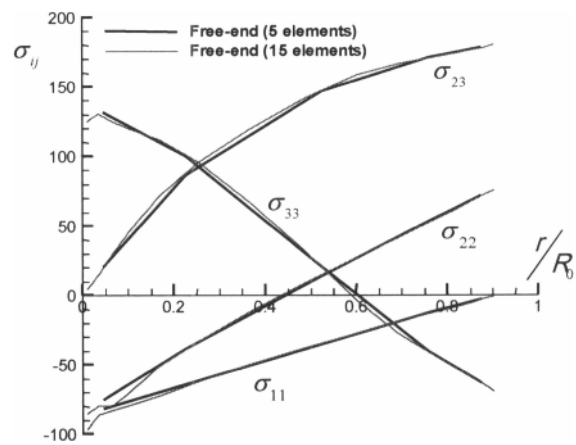

Figure 4. Predicted stress distributions inside the solid bar with the initial random texture under free-end torsion at shear strain $\Gamma = 1.5$ at the outer surface of the bar.

Figure 5 shows the predicted normalized torque $\bar{\tau}$ and axial strain ε as functions of the shear strain Γ for specimens with the initial extrusion texture and random texture. It is found that the predicted response of free-end torsion, especially the axial strain ε, is very sensitive to the initial texture. A noticeable strain softening effect in the $\bar{\tau}$ vs. Γ curves is detected at large strains for both initial textures. For the initial extrusion texture, the predicted axial strain exhibits a complicated trend: contracting first and then elongating axially. This seems in a good qualitative agreement with the experimental axial strain ε vs. Γ curve for the magnesium alloy AZ71 extruded bar under free-end torsion reported by Beausir et al. [11]. For the initial random texture, the predicted axial strain is almost zero up to $\Gamma \approx 0.5$ but becomes very large at large strains.

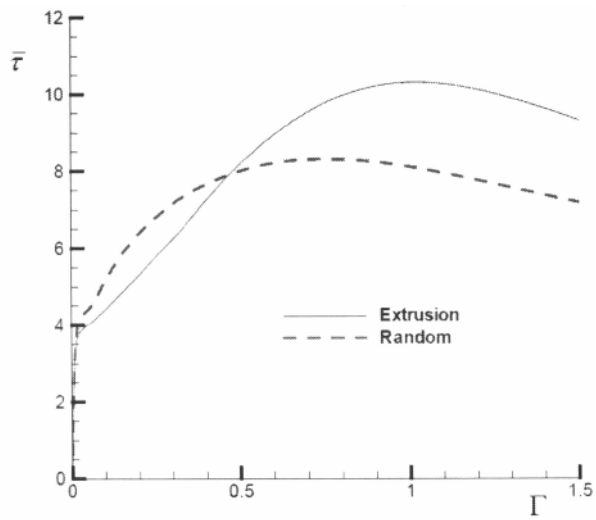

(a)

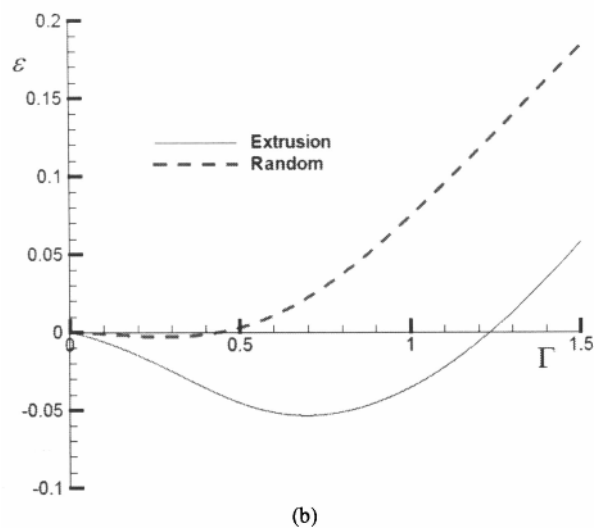

(b)

Figure 5. Predicted normalized torque (a), and elongation (b) for solid bars with the initial extrusion texture and random texture.

Figure 6 shows the predicted deformation textures in terms of $\{0001\}$ and $\{10\bar{1}0\}$ pole figures at $\Gamma = 1.5$ for the initial random and extrusion textures. These pole figures exhibit shear textures analogous to the experimental textures observed in free-end torsion by Beausir et al. [11] for HCP materials. It is also observed that the shear texture from the initial random texture is stronger than the one from the initial extrusion texture.

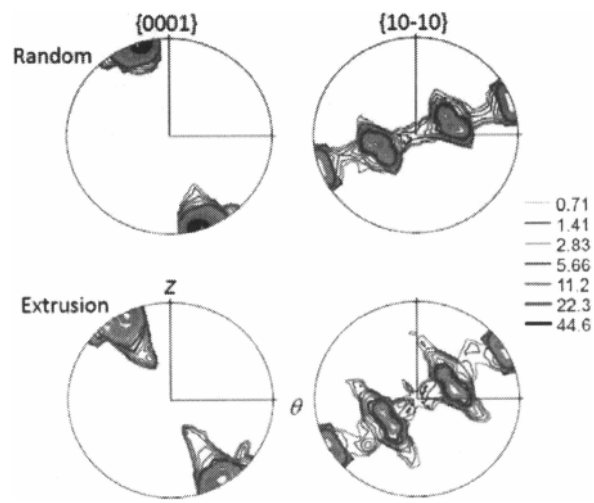

Figure 6. Predicted deformation textures in terms of $\{0001\}$ and $\{10\bar{1}0\}$ pole figures at shear strain $\Gamma = 1.5$ at the outer surface of the bar for the initial random texture (Top) and extrusion texture (Bottom).

The development of the second-order axial strain is believed to mainly result from the initial and deformation induced anisotropy and is thus sensitive to the texture evolution. In this paper, repeating the calculations reported in Fig. 5 but turning off the texture evolution assesses the influence of the texture evolution on free-end torsion. Figures 7 and 8 give the predicted normalized torque and axial strain for the initial extrusion texture and random texture, respectively. In these simulations both texture evolution due to slip and reorientation due to twinning are excluded. It is found that excluding texture evolution dramatically reduces the predicted axial strain. For the initial random texture, the predicted axial strain is nearly zero during the entire deformation process. It is also observed that the softening effect in the $\bar{\tau}$ and Γ curves at large strains is due to texture evolution.

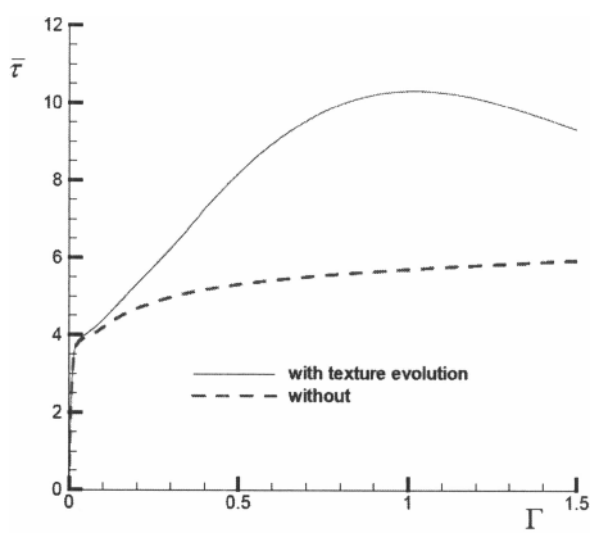

(a)

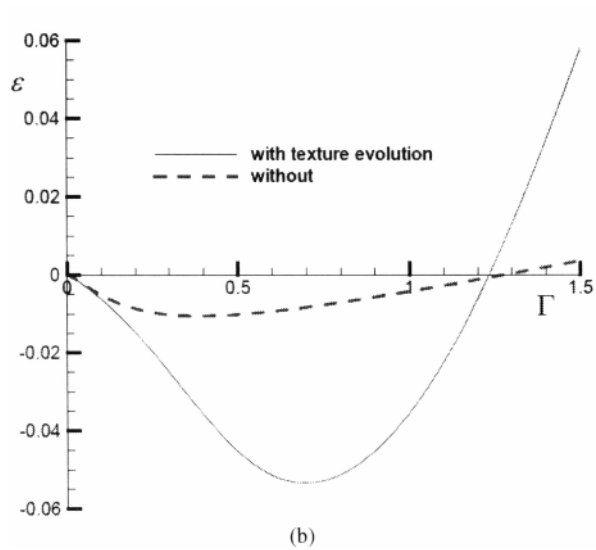

(b)

Figure 7. Predicted effect of texture evolution on normalized torque (a), and elongation (b) for a solid bar with the initial extrusion texture.

Conclusions

In this paper, the large strain free-end torsion of HCP polycrystals has been studied numerically, based on the EVPSC model with the Affine self-consistent scheme. It has been found that the development of the second-order axial strain is very sensitive to the initial anisotropy due to the initial texture, and the deformation induced anisotropy due to the texture evolution. Numerical results have indicated that excluding texture evolution dramatically reduces the development of the axial strain. For the magnesium alloy AZ31 extruded bar, the predicted axial strain exhibits a complicated trend: contracting first and then elongating axially. This is in a good qualitative agreement with the experimental axial response for the magnesium alloy AZ71 extruded bar under free-end torsion reported by Beausir et al. [11]. Numerical results also suggest that the free-end torsion test can provide an effective means for assessing the adequacy of polycrystal plasticity models for magnesium alloys.

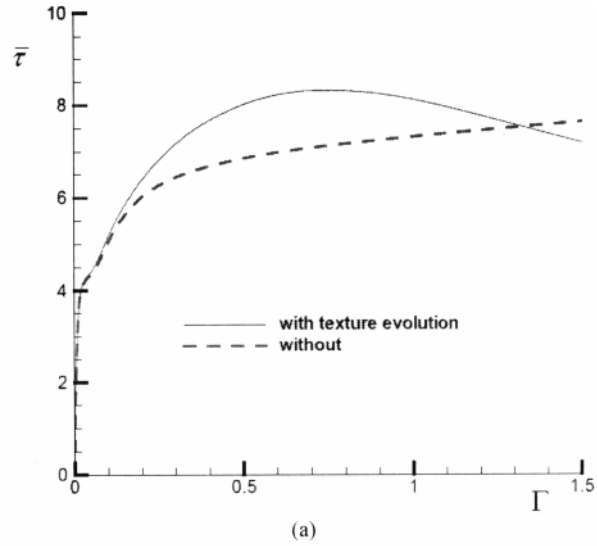

(a)

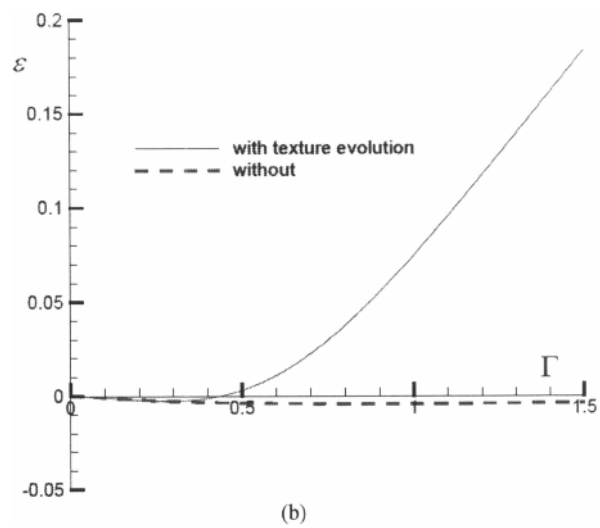

(b)

Figure 8. Predicted effect of texture evolution on normalized torque (a), and elongation (b) for a solid bar with the initial random texture.

Acknowledgement

This research was supported by Ontario Ministry of Research and Innovation and the Natural Sciences and Engineering Research Council of Canada (NSERC).

References

1. H.W. Swift, "Length changes in metals under torsional overstrain," *Engineering*, 163 (1947), 253-257.
2. F. Montheillet, M. Cohen, and J.J. Jonas, "Axial stresses and texture development during the torsion testing of Al, Cu and Alpha-Fe," *Acta Metall.*, 32 (1984), 2077-2089.

3. S. Harren, T.C. Lowe, R.J. Asaro, and A. Needleman, "Analysis of large-strain shear in rate-dependent Face-Centred Cubic polycrystals: Correlation of micro- and macromechanics," *Philosophical Transactions of the Royal Society of London*, A328 (1989), 443-500.
4. K.W. Neale, L.S. Toth, and J.J. Jonas, "Large strain shear and torsion of rate-sensitive FCC polycrystals," *International Journal of Plasticity*, 6 (1991), 45-61.
5. L.S. Toth, J.J. Jonas, D. Daniel, and J.A. Bailey, "Texture development and length changes in copper bars subjected to free end torsion," *Texture and Microstructure*, 19 (1992), 245-262.
6. P.D. Wu, K.W. Neale, and E. Van der Giessen, "Simulation of the behaviour of FCC polycrystals during reversed torsion," *International Journal of Plasticity*, 12 (1996), 1199-1219.
7. P. Sanchez, A. Pochettino, T. Chauveau, and B. Bacroix, "Torsion texture development of zirconium alloys," *Journal of Nuclear Materials*, 298 (2001), 329-339.
8. W.J. Evans, J.P. Jones, and M.T. Whittaker, "Texture effects under tension and torsion loading conditions in titanium alloys," *International Journal of Fatigue*, 27 (2005), 1244-1250.
9. M.R. Barnett, "Influence of deformation condition and texture on the high temperature flow stress of magnesium AZ31," *Journal of Light Metals*, 1 (2001), 167-177.
10. S. Balasubramanian, and L. Anand, "Plasticity of initially textured hexagonal polycrystals at high homologous temperatures: application to titanium," *Acta Materialia*, 50 (2002), 133-148.
11. B. Beausir, L.S. Toth, F. Qods, and K.W. Neale, "Texture and mechanical behavior of magnesium during free-end torsion," *Journal of Engineering Materials and Technology*, 131 (2009), article number 011108.
12. H. Wang, Y. Wu, P.D. Wu, and K.W. Neale, "Numerical analysis of large strain simple shear and fixed-end torsion of HCP polycrystals," *CMC-Computers, Materials & Continua*, 19 (2010), 255-284.
13. K.W. Neale, and S.C. Shrivastava, "Finite elastic plastic torsion of a circular bar," *Engineering Fracture Mechanics*, 21 (1985), 747-754.
14. A. Molinari, G.R. Canova, and S. Ahzi, "A self-consistent approach of the large deformation polycrystal viscoplasticity," *Acta Metallurgica*, 35 (1987), 2983-2994.
15. R.A. Lebensohn, and C.N. Tomé, "A self-consistent anisotropic approach for the simulation of plastic-deformation and texture development of polycrystals - Application to Zirconium alloys" *Acta Metallurgica et Materialia*, 41 (1993), 2611-2624.
16. P.D. Wu, and E. Van der Giessen, "Analysis of elastic-plastic torsion of circular bars at large strains," *Archive of Applied Mechanics*, 61 (1991), 89-103.
17. H. Wang, P.D. Wu, C.N. Tomé, and Y. Huang, "A finite strain elastic-viscoplastic self-consistent model for polycrystalline materials," *Journal of the Mechanics and Physics of Solids*, 58 (2010), 594-612.
18. H. Wang, B. Raeisinia, P.D. Wu, S.R. Agnew, and C.N. Tomé, "Evaluation of self-consistent polycrystal plasticity models for magnesium alloy AZ31B sheet," *International Journal of Solids and Structures*, 47 (2010), 2905-2917.
19. H. Wang, P.D. Wu, and K.W. Neale, "On the role of the constitutive model and basal texture on the mechanical behavior of magnesium alloy AZ31B sheet," *Journal of Zhejiang University – Science*, A11 (2010), 744-755.
20. H. Wang, P.D. Wu, K.P. Boyle, and K.W. Neale, "On crystal plasticity formability analysis for magnesium alloy sheets," *International Journal of Solids and Structures*, 48 (2011), 1000-1010.
21. C.N. Tomé, R.A. Lebensohn, and U.F. Kocks, "A model for texture development dominated by deformation twinning - Application to Zirconium alloys," *Acta Metallurgica et Materialia*, 39 (1991), 2667-2680.
22. P.D. Wu, and E. Van der Giessen, "On large strain inelastic torsion of glassy polymers," *International Journal of Mechanical Sciences*, 35 (1993), 935-951.
23. E. Van der Giessen, P.D. Wu, and K.W. Neale, "On the effect of plastic spin on large strain elastic-plastic torsion of solid bars," *International Journal of Plasticity*, 8 (1992), 773-801.
24. S.R. Agnew, D.W. Brown, and C.N. Tomé, "Validating a polycrystal model for the elastoplastic response of magnesium alloy AZ31 using in situ neutron diffraction," *Acta Materialia*, 54 (2006), 4841-4852.
25. G. Simmons, and H. Wang, *Single crystal elastic constants and calculated polycrystal properties* (Cambridge (MA): MIT Press, 1971).